



**Copolymerisation at work: first example of a highly porous MOF comprising a triarylborane based linker.**

Journal:	<i>CrystEngComm</i>
Manuscript ID:	CE-ART-07-2014-001400.R1
Article Type:	Paper
Date Submitted by the Author:	19-Aug-2014
Complete List of Authors:	Helten, Stella; TU Dresden, Sahoo, Basudev; Uni Münster, Bon, Volodymyr; TU Dresden, Department of Inorganic Chemistry Senkovska, Irena; TU Dresden, Department of Inorganic Chemistry Kaskel, Stefan; Technische Universität Dresden, Institut für Anorganische Chemie Glorius, Frank; Universität Münster, Organisch Chemisches Institut

## ARTICLE

## Copolymerisation at work: first example of a highly porous MOF comprising a triarylborane based linker

Cite this: DOI: 10.1039/x0xx00000x

Stella Helten,<sup>a#</sup> Basudev Sahoo,<sup>b#</sup> Volodymyr Bon,<sup>a</sup> Irena Senkovska,<sup>a</sup> Stefan Kaskel,<sup>a\*</sup> and Frank Glorius<sup>b\*</sup>

Received 00th January 2012,  
Accepted 00th January 2012

DOI: 10.1039/x0xx00000x

www.rsc.org/

Two novel porous materials, namely  $Zn_4O(TPB)_{4/3}(BDC)$  and chiral  $Zn_4O(TPB)_{4/3}(Chir-BDC)$  have been synthesised by copolymerisation of the newly developed triarylborane linker 4,4',4''-boranetriyltris(3,5-dimethylbenzoic acid) ( $H_3TPB$ ) with the linear 1,4-benzene-dicarboxylic acid ( $H_2BDC$ ) or Chir- $H_2BDC$ , respectively. The compounds adopt **1th-d** topology and are microporous. The BET surface area of  $Zn_4O(TPB)_{4/3}(BDC)$  determined from the nitrogen adsorption isotherm measured at 77K is  $2874 \text{ m}^2 \text{ g}^{-1}$  and both frameworks are accessible to organic dye molecules, the largest being Rhodamine B. Thus, the two compounds are the first examples of non-interpenetrated, highly accessible metal-organic frameworks comprising a triarylborane linker. The framework shows an enhanced isosteric heat of  $CO_2$  adsorption in comparison to the isorecticular DUT-6 compound.

### Introduction

Metal-organic frameworks (MOFs) offer a unique chance for the rational design of crystalline, porous materials with designed framework topology and chemical functionality by the virtue of their modular construction from inorganic clusters and organic ligands. This has created sustained research interest in these materials because of the possibilities to tailor the structure and functionality of highly ordered porous solids for several kinds of applications including gas storage,<sup>1</sup> (enantioselective) catalysis<sup>2</sup> and separation in the gas and liquid phase,<sup>3,4,5</sup> and sensing.<sup>6</sup>

One of the advanced features of MOF materials is the possibility for controlled incorporation of a functional organic molecule into a highly ordered porous solid.

However, the engineering of novel crystalline materials with suitable pore systems for a given target molecule is still a big challenge.<sup>7</sup> Copolymerisation of ditopic and tritopic linkers can be a powerful tool not only to prevent framework interpenetration, but also to design MOFs with larger pores and more versatile functionality, compared to the frameworks formed with one of the two linkers alone. This strategy has been successfully demonstrated for several compounds with MOFs featuring different linear ditopic linkers combined with a tritopic linker (UMCM-1-5, DUT-6, MOF-210) or with tritopic and tetratopic linkers (DUT-25).<sup>8,9,10</sup> Also, incorporation of three different ligands in one structure was reported recently.<sup>11</sup>

Triarylboranes have attractive properties, such as fluorescence<sup>12</sup> and strong Lewis acidity. Recently, Kleitz, Wang and co-workers reported the first example of a MOF (B-MOF) comprising a triarylborane linker with carboxylate donor groups.<sup>13</sup> B-MOF-1 has an eightfold interpenetrated framework with very limited porosity and pore accessibility. Also, MOFs including only triarylamine linkers and Zn(II) as SBU-forming metal-ion tend to form rather dense structures.<sup>14,15,16</sup> Both triarylborane and triarylamine molecules display a similar propeller-like twisting around the core heteroatom and can therefore be considered as geometrically similar.

Our efforts are focused on the synthesis of non-interpenetrated porous triarylborane based MOFs. For this purpose, a new linker 4,4',4''-boranetriyltris(3,5-dimethylbenzoic acid) ( $H_3TPB$ , Fig. 2a) was developed and the copolymerisation route was chosen as the synthetic strategy. When  $H_2BDC$  was utilised in the synthesis as a second ditopic co-linker, crystals of  $Zn_4O(TPB)_{4/3}(BDC)$  (**1**) were obtained. Zinc nitrate,  $H_3TPB$  and  $H_2BDC$  were reacted in a ratio of 4.0:0.3:1 in DEF at 80 °C.

Single crystal X-ray analysis shows that the structure belongs to the cubic  $Pm-3n$  space group with the cell parameter  $a = 26.510 \text{ \AA}$ . As SBU, one crystallographically independent  $Zn_4O$  cluster is present and both linkers (BDC and TPB) are incorporated into the structure. The asymmetric unit contains one zinc atom (Zn1) in  $24k$  and one oxygen atom (O3) in  $6d$  Wyckoff positions (which by the implementation of two-fold

axis and mirror plane give  $Zn_4O$  cluster), a quarter of BDC ligand (represented by one oxygen atom O2 and three carbon atoms C7, C8, and C9) and a sixth part of TPB ligand (represented by B1, C1, C2, C5, and O1). The inversion center, together with one of the three mirror planes that intersect in the  $6b$  Wyckoff position ensured the generation of the BDC ligand. The all atoms of TPB ligand are generated by the combination of 3-fold axis, passing through the B1 atom, located in  $8e$  Wyckoff position and 2-fold axis, perpendicular to the 3-fold one and passing through C1, C2, C5 and B1 atoms.

As already discussed, the topology of a MOF containing ditopic (D) and tritopic (T) linkers and  $Zn_4O$  clusters is determined by the ratio D:T and by the arrangement of these linkers around that SBU.<sup>8,17</sup> In the case of **1**, four trigonal TPB linkers are positioned in the equatorial plane of the octahedral SBU, while the two linear BDC linkers occupy the two axial positions (D:T = 2:4). (Fig. 1)

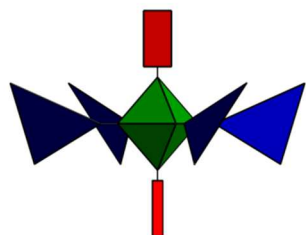


Fig. 1: Schematic representation of the arrangement of the ditopic linkers (red) and the tritopic linkers (blue) at the SBU (green)

This arrangement of the linkers around the  $Zn_4O$ -SBU leads to an **ith-d** topology previously realised in the isorecticular compound DUT-6 (MOF-205).<sup>9</sup> Notably, the ratio between the distance of the carboxylate C atoms within the ditopic and trigonal linkers ( $L_d/L_T$ ) amounts to 0.544 in **1** and 0.645 in DUT-6 (determined from crystal structures, Fig. 2).

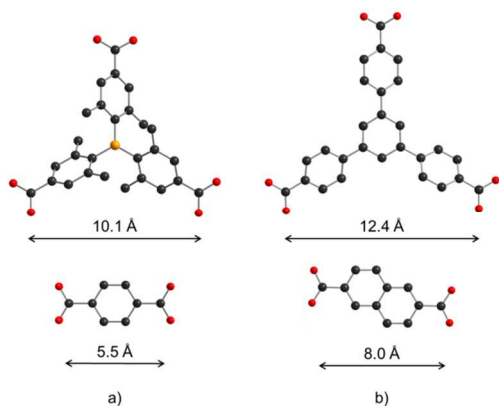


Fig. 2: Comparison of distances between carbon atoms of carboxyl groups in: a) **1** and b) DUT-6

Interestingly, UMCM-4, a MOF constructed from a triarylamine based linker and BDC ( $L_d/L_T = 0.577$ ), adopts a different topology. However, in the case of UMCM-4, the D:T ratio is 3:3. When applying the synthetic feed ratios reported

for UMCM-4 formation, no analogue of UMCM-4 was formed in any of the syntheses trials. Later, the linker ratio was subsequently optimised for the formation of phase pure **1**. It must be noted, that the angle between the planes spanned by the phenyl rings of the two tritopic linkers are different: while the angles in the triarylamine linker are  $72.5^\circ$ ,  $65.4^\circ$  and  $68.5^\circ$  in UMCM-4, the attached methyl groups force the phenyl rings of TPB further apart, resulting in an angle of  $88.4^\circ$  between all respective phenyl rings in **1**. This subtle difference obviously has an influence on MOF formation.

As in DUT-6, there are two types of pores present in the framework of **1**: a dodecahedral pore built up from four linear and eight trigonal linkers interconnecting twelve  $Zn_4O$  clusters; and a tetrahedral pore built up from four  $Zn_4O$  clusters interconnected by two linear and four trigonal linkers (Fig. 3).

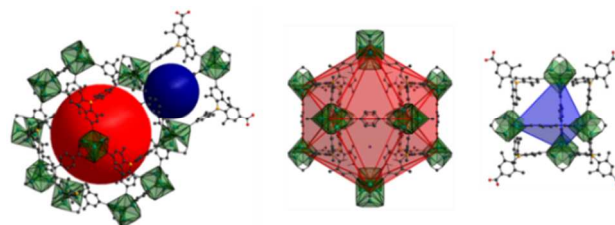


Fig. 3: Representation of pores within the framework; red, dodecahedral pore; blue, tetrahedral pore

The pore windows are each bordered by three  $Zn_4O$  clusters interconnected by two trigonal and one linear linker.

The shorter linkers make **1** a purely microporous compound: in **1**, the pore diameters are  $15 \text{ \AA}$  for the dodecahedral pore,  $10 \text{ \AA}$  for the tetrahedral pore, and  $5 \text{ \AA}$  for the pore windows (taking Van der Waals radii into account). By contrast, the analogue dimensions in the mesoporous DUT-6 are  $22 \text{ \AA}$ ,  $8 \text{ \AA}$  and  $7 \text{ \AA}$  in diameter. The seeming discrepancy in the size ratio of the tetrahedral pores of the two isorecticular compounds arises from the larger steric demand of the ditopic NDC linker in DUT-6.

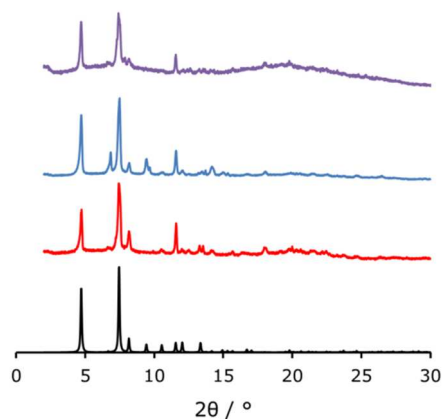


Fig. 4: Powder X-ray diffraction patterns: in black - theoretical calculated from the crystal structure of **1**; in red - as synthesised compound **1**; in blue - **1** activated by drying with supercritical  $CO_2$ ; in violet - as synthesised **2**.

To confirm the microporosity, nitrogen physisorption experiments at  $77 \text{ K}$  were performed on the activated sample. As conventional activation after solvent exchange to ethanol or

dichloromethane resulted in framework collapse, drying with supercritical CO<sub>2</sub> was utilised to achieve gentle desolvation of the framework.

A good agreement between the calculated X-ray diffraction pattern and the PXRD of the synthesised compound clearly shows the phase purity as well as the preservation of the crystallinity in the supercritically activated **1** (Fig. 4).

As expected from the crystal structure, **1** displays a Type I physisorption isotherm for N<sub>2</sub> at 77 K (Fig. 5).

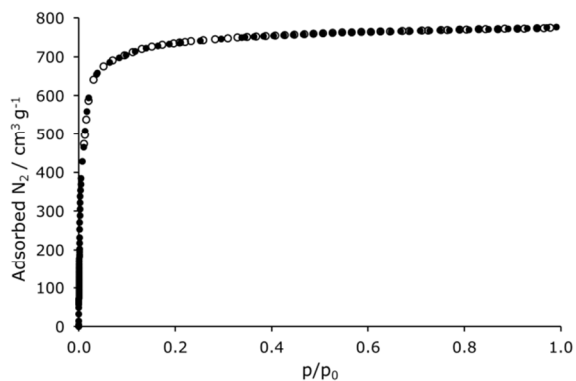


Fig. 5: Nitrogen physisorption isotherm at 77 K, solid symbols represent adsorption, hollow symbols represent desorption.

The N<sub>2</sub> uptake at saturation is 776 cm<sup>3</sup> g<sup>-1</sup> resulting in the pore volume of 1.20 cm<sup>3</sup> g<sup>-1</sup> ( $p/p_0 = 0.99$ ). The BET surface area of the compound was determined using the adsorption branch with  $7.7 \times 10^{-4} \leq p/p_0 \leq 9.8 \times 10^{-2}$  fulfilling the three consistency criteria proposed by Rouquerol et al.<sup>18</sup> (†ESI S2) and amounts to 2874 m<sup>2</sup> g<sup>-1</sup>. Thus, Zn<sub>4</sub>O(TPB)<sub>4/3</sub>(BDC) is the first example of a highly porous MOF comprising a triarylborane based linker. Carbon dioxide adsorption at 194.5 K and 273 K was applied to study the interaction of CO<sub>2</sub> molecules with the MOF surface (Fig. 6).

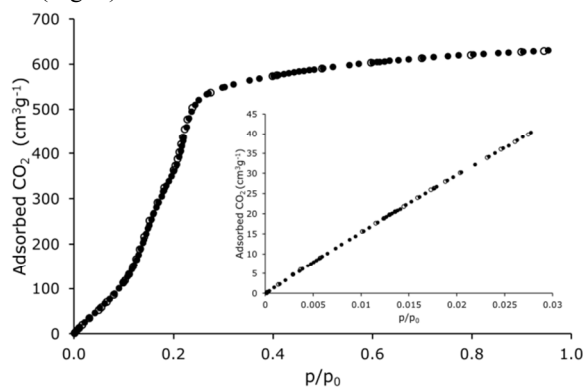


Fig. 6: CO<sub>2</sub> physisorption isotherms at 194.5 K; inlet, black symbols, CO<sub>2</sub> physisorption isotherm at 273 K

The isosteric heat of adsorption ( $Q_{st}$ ) could be calculated using the Clausius–Clapeyron equation as a function of the adsorbed amount of CO<sub>2</sub>. Saturation uptake at 194.5 K is 630.58 cm<sup>3</sup> g<sup>-1</sup> and the uptake at 1 bar and 273 K is 40.327 cm<sup>3</sup> g<sup>-1</sup>. The collected data allows calculation of the isosteric heat of adsorption by coverage from 0.036 mmol/g to 1.8 mmol/g. At

the lowest coverage the isosteric heat of adsorption amounts to 21.5 kJ mol<sup>-1</sup> and decreases to 18.3 kJ mol<sup>-1</sup> at higher coverage (Fig. 7).

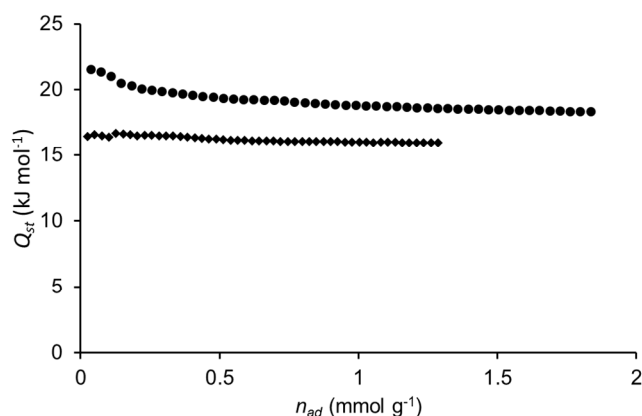


Fig. 7: Isosteric heats of adsorption for **1** (circles) and DUT-6 (diamonds).

The value at low coverage in particular is higher compared to experimentally determined isosteric heats of adsorption for other Zn<sub>4</sub>O based MOFs at low or near zero coverage: 16.7 kJ mol<sup>-1</sup> for the heteroatom free isorecticular compound DUT-6 (Fig. 7, for adsorption isotherms see †ESI, S5), 15 kJ mol<sup>-1</sup> for MOF-5, 16.8–19.2 kJ mol<sup>-1</sup> (depending on experimental method) for IRMOF-3,<sup>19</sup> 11.9 kJ mol<sup>-1</sup> for UCMC-1<sup>20</sup> and 14 kJ mol<sup>-1</sup> for MOF-177 (uniformly determined for all coverages)<sup>21</sup> pointing on the specific interaction sites within the framework. This value is comparable with those observed for MOFs containing open metal sites (21–47 kJ mol<sup>-1</sup>), but is considerably lower than values reported for amine functionalized materials (38–96 kJ mol<sup>-1</sup>).<sup>22,23</sup> To further increase the CO<sub>2</sub> surface interaction, the synthesis of a compound containing triarylborane linker and amino functionalised BDC will be beneficial.

The tolerance of the structure towards the incorporation of functionalised terephthalic acid was demonstrated using chirally modified BDC. As shown recently, the Chir-BDC linker can be easily incorporated into the UCMC-1 structure by replacing BDC by Chir-BDC in the synthesis. This route allows for the design of chiral MOFs with desired topology and pore dimensions. Chir-BDC (in this case (*S*)-2-(4-benzyl-2-oxazolidin-2-yl) substituted BDC) was synthesised according to the previously reported procedure.<sup>24</sup> Using a similar synthesis procedure, crystals of Zn<sub>4</sub>O(TPB)<sub>4/3</sub>(Chir-BDC) (**2**) could be obtained. The PXRD patterns confirm the isorecticular structure of **1** and **2** (Fig. 4).

Since accessibility of larger substrate molecules is important for many desired applications of chiral MOFs (such as for enantiomer separation), the adsorption of organic dye molecules (Methylene Blue, Brilliant Green, Rhodamine B, and Reichardt's dye) was performed. All of the above mentioned dyes, with the exception of Reichardt's Dye could enter the frameworks of both compounds in the liquid phase, resulting in colouring of the crystals (†ESI S4).

Photophysical characterisation of H<sub>3</sub>TPB and **1** shows blue fluorescence with a bathochromic shift in the maximum of the emission wavelength of **1** ( $\lambda = 443$  nm) in respect to H<sub>3</sub>TPB ( $\lambda = 402$  nm) (†ESI, S7).

## Conclusions

Copolymerisation of a triarylborane tricarboxylate linker with the linear ditopic H<sub>2</sub>BDC or its chiral derivative has afforded the first non-interpenetrated highly accessible triarylborane containing metal-organic frameworks with an **ith-d** topology. Accessibility of the two compounds for larger probe molecules could be confirmed by dye adsorption. Zn<sub>4</sub>O(TPB)<sub>4/3</sub>(BDC) could be successfully activated and the BET area determined from the nitrogen adsorption isotherm is 2874 m<sup>2</sup> g<sup>-1</sup>, surpassing by far the surface area for previously reported borane containing MOFs. The microporous character as well as Lewis acidity of the tri-coordinate boron atom of the linker contribute to the high isosteric heat of CO<sub>2</sub> adsorption at low coverage. The blue fluorescence of H<sub>3</sub>TPB is preserved in the porous compound.

Thus, the incorporation of two prominent attributes of triarylboranes, namely Lewis acidity and fluorescence, into a highly accessible porous crystalline material could be successfully demonstrated.

## Acknowledgements

The authors are grateful for the financial support from the DFG (SPP 1362) and the HZB. Special thanks goes to the Dr. M. S. Weiss (BESSY, Berlin) for support during the single crystal measurements. B.S. thanks NRW Graduate School of Chemistry for their support.

## Experimental

### Materials and methods

Unless otherwise indicated, commercially obtained chemicals were used as received. Zn(NO<sub>3</sub>)<sub>2</sub> · 4 H<sub>2</sub>O (98.5% purity) was purchased from Merck. Terephthalic acid (99% purity) was purchased from Acros Organics. (*S*)-2-(4-Benzyl-2-oxazolidin-3-yl)terephthalic acid was synthesized according to the published procedure.<sup>24</sup> N,N-Diethylformamide (99% purity) was purchased from SAFC Global. Ethanol (analytical reagent grade) was purchased from Fisher Scientific. Detailed information about the synthesis of 4,4',4''-boranetriyltris(3,5-dimethylbenzoic acid) and reagents used in this synthesis is given in †ESI, S1.

Powder X-Ray Diffraction data was collected on a STADI P diffractometer with Cu-K $\alpha$ 1 radiation ( $\lambda = 1.5405$  Å) at room temperature. Thermogravimetric Analysis was carried out on a STA 409 (Netzsch) with a heating rate of 5 K min<sup>-1</sup> and synthetic air as carrier gas with a flow rate of 100 mL min<sup>-1</sup>.

Nitrogen physisorption experiments were performed on a BELSORP-max (Bel, Japan) at 77 K up to 1 bar. CO<sub>2</sub> physisorption measurements were performed on a BELSORP-

max (Bel, Japan) at 195 K and 273 K up to 1 bar. C,H,N elemental analyses were performed on a CHNS 932 analyser (LECO). Liquid UV-Vis measurements were carried out on a UV-1650PC spectrophotometer (Shimadzu). Solid state UV-Vis measurements were performed on a Cary 4000 UV-Vis Spectrophotometer with praying mantis geometry using PTFE as white standard. Both liquid and solid state fluorescence measurements were conducted on a Cary Eclipse fluorescence spectrophotometer.

### Single crystal X-ray diffraction experiments

The dataset from the single crystal of Zn<sub>4</sub>O(TPB)<sub>4/3</sub>(BDC), prepared in a glass capillary, was collected at beamline BL14.2, Joint Berlin-MX Laboratory of Helmholtz Zentrum Berlin, equipped with a MX-225 CCD detector (Rayonics, Illinois) and 1-circle goniometer.<sup>25</sup> The data collection was performed at room temperature using monochromatic radiation with  $\lambda = 0.88561$  Å. A plethora of single crystals from different batches with various linear dimensions (up to 0.5 mm in all dimensions) were used for single crystal diffraction experiments at room temperature and at 100 K. In spite of sufficient size of single crystals and highly intensive synchrotron radiation, the sufficient intensities could be observed up until a resolution of 1.0 – 1.1 Å. The indexing of the image frames suggests a primitive cubic lattice for the crystal structure. The image frames were integrated and scaled using XDSAPP 1.0<sup>26</sup> graphic shell for the XDS program.<sup>27</sup> The obtained set of intensities was carefully analyzed on extinction. As a result, systematic absences were found for the glide plane, perpendicular to the face diagonal, suggesting the *Pm-3n* space group for the crystal structure solution and refinement. The structure was solved by direct methods and refined by full-matrix least square on F<sup>2</sup> using SHELXS and SHELXL<sup>28</sup> programs respectively. All non-hydrogen atoms were refined in the anisotropic approximation. Hydrogen atoms were generated geometrically regarding the hybridization of the parent atom and refined using the “riding model” with U<sub>iso</sub>(H) = 1.5 U<sub>iso</sub>(C) for CH<sub>3</sub> and U<sub>iso</sub>(H) = 1.2 U<sub>iso</sub>(C) for CH groups. The anisotropic refinement decreased the data to parameter ratio for the observed reflections that had a strong influence on the refinement stability from the dataset with mean I/ $\sigma$ (I) = 2.36. This prompted us to use 11 distance restraints to fix the geometry of the organic ligands. Besides that, lattice solvent molecules could not be located from the difference Fourier map due to disorder in the highly symmetrical space group. Thus, the SQUEEZE procedure in PLATON was performed to correct the intensities, corresponding to the disordered part of the structure.<sup>29</sup> This results in 5202 electrons squeezed from 13642 Å<sup>3</sup> that corresponds to 15.5 molecules of DEF per formula unit. CCDC-1009603 contains the supplementary crystallographic data for this paper. This data can be obtained free of charge from the Cambridge Crystallographic Data Centre via [www.ccdc.cam.ac.uk/data\\_request/cif](http://www.ccdc.cam.ac.uk/data_request/cif).

### Synthesis of Zn<sub>4</sub>O(C<sub>8</sub>H<sub>4</sub>O<sub>4</sub>)(C<sub>27</sub>H<sub>24</sub>BO<sub>6</sub>)<sub>4/3</sub>

Zn(NO<sub>3</sub>)<sub>2</sub>•4 H<sub>2</sub>O (56 mg, 0.2 mmol), terephthalic acid (9 mg, 0.054 mmol) and 4,4',4''-boranetriyltris(3,5-dimethylbenzoic acid) (8.1 mg, 0.018 mmol) were dissolved in N,N-diethylformamide (10 mL) by ultrasonication. The solution was placed in a glass Pyrex tube with a size of 100 x 16 mm. The vial was sealed with a screw cap and heated at 80 °C in an oven for 48 hours. After cooling down to room temperature, the mother liquor was pipetted off and the colourless crystals were washed with fresh DEF five times. The solvent was then exchanged with ethanol five times. 24 hours were left between consecutive washing and solvent exchange steps.

For physisorption measurements, the ethanol was removed from the pores by drying in supercritical CO<sub>2</sub>.

Elemental analysis: Calculated for Zn<sub>4</sub>O(C<sub>8</sub>H<sub>4</sub>O<sub>4</sub>)(C<sub>27</sub>H<sub>24</sub>BO<sub>6</sub>)<sub>4/3</sub>: C, 50.39%; H, 3.46%; Measured: C, 49.92%; H, 3.73%

#### Synthesis of Zn<sub>4</sub>O(C<sub>17</sub>H<sub>13</sub>NO<sub>6</sub>)(C<sub>27</sub>H<sub>24</sub>BO<sub>6</sub>)<sub>4/3</sub>

Zn(NO<sub>3</sub>)<sub>2</sub>•4 H<sub>2</sub>O (60 mg, 0.2 mmol), (S)-2-(4-Benzyl-2-oxazolidin-3-yl)terephthalic acid (0.028 mg, 0.048 mmol) and 4,4',4''-boranetriyltris(3,5-dimethylbenzoic acid) (13 mg, 0.028 mmol) were dissolved in N,N-Diethylformamide (10 mL) by ultrasonication. The vial was sealed by a screw cap and heated at 80 °C in an oven for 48 hours. After cooling down to room temperature, the mother liquor was pipetted off and replaced by fresh DEF five times. The solvent was then exchanged with ethanol five times. 24 Hours were left between consecutive washing and exchange steps.

#### Notes and references

<sup>a</sup> Dresden University of Technology

Institute for Inorganic Chemistry

Bergstr. 66

01069 Dresden

e-mail: Stefan.Kaskel@chemie.tu-dresden.de

<sup>b</sup>Westfälische Wilhelms-Universität Münster

NRW Graduate School of Chemistry

Organisch-Chemisches Institut

Corrensstr. 40

48149 Münster

e-mail: glorius@uni-muenster.de

<sup>#</sup>These authors contributed equally to this work

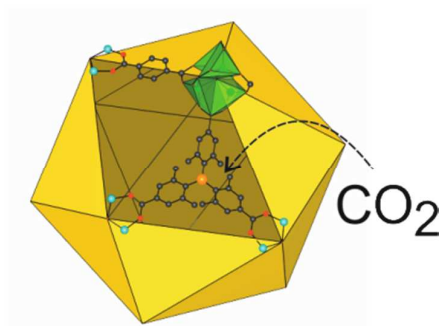
† **Crystal data for Zn<sub>4</sub>O(TPB)<sub>4/3</sub>(BDC)·15.5DEF:** C<sub>121.5</sub>H<sub>206.5</sub>B<sub>1.33</sub>N<sub>15.5</sub>O<sub>28.5</sub>Zn<sub>4</sub>, *M* = 2616.40 g mol<sup>-1</sup>, cubic, *Pm*-3*n* (Nr. 223), *a* = 26.510(3) Å, *V* = 18631(6) Å<sup>3</sup>, *Z* = 6, *ρ*<sub>calc</sub> = 1.399 g cm<sup>-3</sup>, *λ* = 0.88561 Å, *T* = 293 K, *θ*<sub>max</sub> = 25.4°, reflections collected/unique 11962/1506, *R*<sub>int</sub> = 0.0497, *R*<sub>1</sub> = 0.1167, *wR*<sub>2</sub> = 0.3864, *S* = 1.109, largest diff. peak 0.183 e Å<sup>-3</sup> and hole -0.774 e Å<sup>-3</sup>. CCDC-1009603 contains the supplementary crystallographic data for this paper. These data can be obtained free of charge from the Cambridge

Crystallographic Data Centre via [www.ccdc.cam.ac.uk/data\\_request/cif](http://www.ccdc.cam.ac.uk/data_request/cif).

Electronic Supplementary Information (ESI) available: [Synthesis of H<sub>3</sub>TPB, Determination of BET area, Thermogravimetric analysis, Dye adsorption, CO<sub>2</sub> adsorption isotherms for DUT-6, Photophysical properties of H<sub>3</sub>TPB and 1]. See DOI: 10.1039/b000000x/

1. K. Konstas, T. Osl, Y. Yang, M. Batten, N. Burke, A. J. Hill, and M. R. Hill, *J. Mater. Chem.*, 2012, **22**, 16698.
2. J. Lee, O. K. Farha, J. Roberts, K. a Scheidt, S. T. Nguyen, and J. T. Hupp, *Chem. Soc. Rev.*, 2009, **38**, 1450–9.
3. Z. Zhang, Y. Zhao, Q. Gong, Z. Li, and J. Li, *Chem. Commun. (Camb)*, 2013, **49**, 653–61.
4. H. Wu, Q. Gong, D. H. Olson, and J. Li, *Chem. Rev.*, 2012, **112**, 836–68.
5. G. Nickerl, A. Henschel, R. Grünker, K. Gedrich, and S. Kaskel, *Chemie Ing. Tech.*, 2011, **83**, 90–103.
6. L. E. Kreno, K. Leong, O. K. Farha, M. Allendorf, R. P. Van Duyne, and J. T. Hupp, *Chem. Rev.*, 2012, **112**, 1105–25.
7. M. G. Goesten, F. Kapteijn, and J. Gascon, *CrystEngComm*, 2013, **15**, 9249.
8. K. Koh, A. G. Wong-Foy, and A. J. Matzger, *J. Am. Chem. Soc.*, 2010, **132**, 15005–10.
9. N. Klein, I. Senkowska, K. Gedrich, U. Stoeck, A. Henschel, U. Mueller, and S. Kaskel, *Angew. Chem. Int. Ed. Engl.*, 2009, **48**, 9954–7.
10. R. Grünker, V. Bon, A. Heerwig, N. Klein, P. Müller, U. Stoeck, I. a Baburin, U. Mueller, I. Senkowska, and S. Kaskel, *Chemistry*, 2012, **18**, 13299–303.
11. L. Liu, K. Konstas, M. R. Hill, and S. G. Telfer, *J. Am. Chem. Soc.*, 2013, **135**, 17731–4.
12. P. C. A. Swamy and P. Thilagar, *Inorg. Chem.*, 2014, **53**, 2776–86.
13. B. a Blight, R. Guillet-Nicolas, F. Kleitz, R.-Y. Wang, and S. Wang, *Inorg. Chem.*, 2013, **52**, 1673–5.
14. H. K. Chae, J. Kim, O. D. Friedrichs, M. O'Keeffe, and O. M. Yaghi, *Angew. Chem. Int. Ed. Engl.*, 2003, **42**, 3907–9.
15. E. Y. Lee, S. Y. Jang, and M. P. Suh, *J. Am. Chem. Soc.*, 2005, **127**, 6374–81.
16. M. P. Suh, Y. E. Cheon, and E. Y. Lee, *Chemistry*, 2007, **13**, 4208–15.
17. R. Grünker, V. Bon, P. Müller, U. Stoeck, S. Krause, U. Mueller, I. Senkowska, and S. Kaskel, *Chem. Commun. (Camb)*, 2014, **50**, 3450–2.

18. J. Rouquerol, P. Llewellyn, and F. Rouquerol, in *Characterization of Porous Solids VII Proceedings of the 7th International Symposium on the Characterization of Porous Solids (COPS-VII), Aix-en-Provence, France, 26-28 May 2005*, eds. J. R. P.L. Llewellyn F. Rodriguez-Reinoso and N. Seaton, Elsevier, 2007, vol. 160, pp. 49–56.
19. D. Farrusseng, C. Daniel, C. Gaudillère, U. Ravon, Y. Schuurman, C. Mirodatos, D. Dubbeldam, H. Frost, and R. Q. Snurr, *Langmuir*, 2009, **25**, 7383–8.
20. B. Mu, P. M. Schoenecker, and K. S. Walton, *J. Phys. Chem. C*, 2010, **114**, 6464–6471.
21. J. a. Mason, K. Sumida, Z. R. Herm, R. Krishna, and J. R. Long, *Energy Environ. Sci.*, 2011, **4**, 3030.
22. R. Babarao and J. Jiang, *Langmuir*, 2008, **24**, 6270–8.
23. Q. Yang, C. Zhong, and J. Chen, *J. Phys. Chem. C*, 2008, **112**, 1562–1569.
24. M. Padmanaban, P. Müller, C. Lieder, K. Gedrich, R. Grünker, V. Bon, I. Senkowska, S. Baumgärtner, S. Opelt, S. Paasch, E. Brunner, F. Glorius, E. Klemm, and S. Kaskel, *Chem. Commun. (Camb.)*, 2011, **47**, 12089–91.
25. U. Mueller, N. Darowski, M. R. Fuchs, R. Förster, M. Hellmig, K. S. Paithankar, S. Pühringer, M. Steffien, G. Zoicher, and M. S. Weiss, *J. Synchrotron Radiat.*, 2012, **19**, 442–9.
26. M. Krug, M. S. Weiss, U. Heinemann, and U. Mueller, *J. Appl. Crystallogr.*, 2012, **45**, 568–572.
27. W. Kabsch, *Acta Crystallogr. D. Biol. Crystallogr.*, 2010, **66**, 125–32.
28. G. M. Sheldrick, *Acta Crystallogr. A.*, 2008, **64**, 112–22.
29. A. L. Spek, *Acta Crystallogr. D. Biol. Crystallogr.*, 2009, **65**, 148–55.



A copolymerization approach was successfully utilized to create the first highly accessible, non-interpenetrated MOF comprising a triarylborane carboxylate linker.